

Six-fold rotationally symmetric vanadium oxide nanostructures by a morphotropic phase transition

C. O'Dwyer^{*,1}, V. Lavayen^{1,2}, D. Fuenzalida^{2,3}, S. B. Newcomb⁴, M. A. Santa Ana¹, E. Benavente³, G. González², and C. M. Sotomayor Torres¹

¹ Tyndall National Institute, University College Cork, Cork, Ireland

² Departamento de Química, Facultad de Ciencias, Universidad de Chile, P.O. Box 653, Santiago, Chile

³ Department of Chemistry, Universidad Tecnológica Metropolitana, P.O. Box 9845, Santiago, Chile

⁴ Glebe Scientific Ltd., Newport, Co. Tipperary, Ireland

Received 12 April 2007, accepted 28 July 2007

Published online 26 September 2007

PACS 61.10.Nz, 61.14.Lj, 61.46.-w, 68.37.Hk, 81.16.Be, 81.30.-t

In this work, we report the first observation of unique hierarchical six-fold rotational symmetrical vanadium oxide based nanocomposite synthesized by a simple chemical route and highlight the first observation of a morphotropic reconstructive phase transition from a lamellar V_2O_5 to that of a single crystalline V_6O_{11} nanostructure.

© 2007 WILEY-VCH Verlag GmbH & Co. KGaA, Weinheim

1 Introduction

Considerable attention is now being directed to transition metal nanostructures, such as VO_x and ZnO, for example [1], based on their metal oxides [2, 3] which, due to their versatile chemical properties often modulable by changes in the oxidation state of the metal coordination sphere, may lead to a variety of products and tunable materials [4, 5]. From the lamellar V_2O_5 xerogel [6], numerous two dimensional organic–inorganic intercalation products have been obtained [7].

In this report of unique hierarchical six-fold rotational symmetrical vanadium oxide based nanocomposite synthesized by a simple chemical route, structures were realised without the use of a catalyst. This method exploits the combination of surfactant/inorganic self-assembly processes and host/guest intercalation chemistry to obtain anisotropic recrystallization of the vanadium oxide directly from its xerogel. A morphotropic reconstructive phase transition occurs during hydrothermal treatment rendering a V_6O_{11} single crystal nanostructure. Each nanostructure is composed of six spoke-like V_6O_{11} platelets of near-equal dimensions and crystal orientation. We examine the anisotropic 1D–3D structural evolution and elucidate the specifics of the shape-determining process.

2 Experimental

To synthesize the product, 5 ml of an aqueous solution of V_2O_5 xerogel (0.43×10^{-3} mol $V_2O_5 \cdot 1.5H_2O$) was treated with dodecanethiol by heating at 313 K for 2 h. After addition of 10 ml ethanol/ H_2O (1:1 v/v) the mixture was vigorously stirred for 48 h at 313 K. Approximately 3 ml of resulting dark green, gel-like suspension were then transferred to a Teflon-lined autoclave and heated under auto generated pressure at 453 K for several days. From obtained suspension a dark solid was separated, washed

* Corresponding author: e-mail: codwyer@tyndall.ie, Phone: +353 21 4904391, Fax: +353 21 4904467

with water and ethanol and dried under vacuum (10^{-3} mm Hg) for 48 h. The final product corresponds to a 98.53% pure vanadate containing 1.34% dodecanethiol and 0.13% sulphur. Analysis calculated for $C_{0.15}H_{0.75}S_{0.02}O_{5.21}V_2$: C (0.955), H (0.346), S (0.34); Exp: C (0.956), H (0.396), S (0.347). After hydrothermal treatment, the resulting crystals are from the so-called vanadium Magnéli phases, defined by V_nO_{2n-1} ($3 \leq n \leq 9$) giving rise to a homologous series of compounds with closely related crystal structures where oxygen atoms form a distorted hexagonal-close-packed array [8].

The morphological characterization of the nanostructured products was performed by field emission scanning electron microscopy (FESEM) using a JEOL JSM-6700F operating at beam voltages between 1–10 kV. Electron transparent specimens were prepared by ion-milling techniques and placed on a holey carbon support. Transmission electron microscopy (TEM) and selected area electron diffraction (SAED) were conducted using a JEOL 2000FX operating at 200 kV.

3 Results and discussion

The morphology of the samples was studied using FESEM. The characteristic cog-like architecture of the as-synthesized structures is clearly shown in Fig. 1a. We observe a high degree of relative uniformity for each of the structures in the synthesized product, and quantities of several grammes are easily obtained from the synthesis procedure. Each structures has an average size of $1.5 \mu\text{m}$ where the diameter of the central core is ~ 500 nm and the length of each platelet measured from the outer edge of the core is also ~ 500 nm. More detailed studies of the structural dimensions were provided by TEM. A typical region of the sample is shown at relatively low magnification in Fig. 1b where an individual nanostructure is observed. Each structure exhibits three axes of symmetry and contains the six platelets marked at A–F that protrude from the central axis. The $\sim 60^\circ$ angle between each pair of platelets corresponds to six-fold rotational symmetry in the c plane. It should be noted that the relatively high thickness of the branches forming the platelet A, for example, arises from the fact that the particle is lying at an angle to the incident electron beam. Selected area electron diffraction measurements in Figs. 1 and 2 confirm the single-crystalline V_6O_{11} phase of the nanostructures with reconstructed lattice parameters of $a_0 = 0.544$ nm, $b_0 = 0.699$ nm and $c_0 = 2.366$ nm; space group (SG) = $P\bar{1}$.

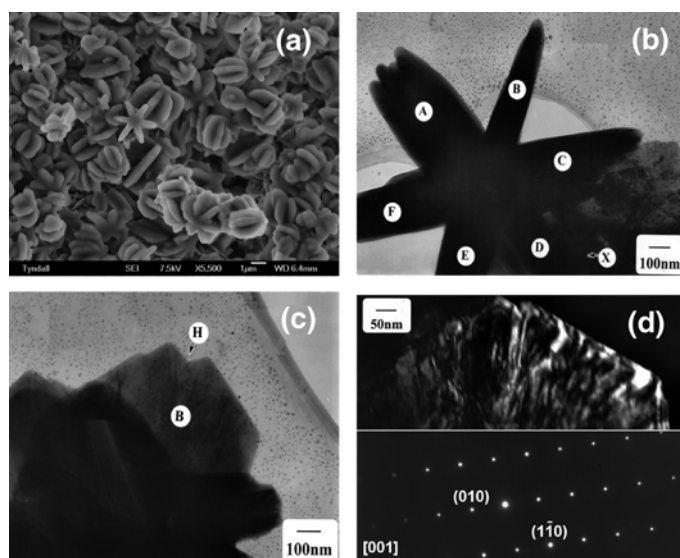


Fig. 1 (a) FESEM micrograph of the as-synthesized nanostructures. (b) TEM image of an individual structure with the six platelets labelled A–F. (c) TEM image of a single platelet after tilting (b) in the direction marked X. (d) SAED pattern of an individual platelet along its $[7\ 9\ 1]$ zone normal of the (001) face of V_6O_{11} .

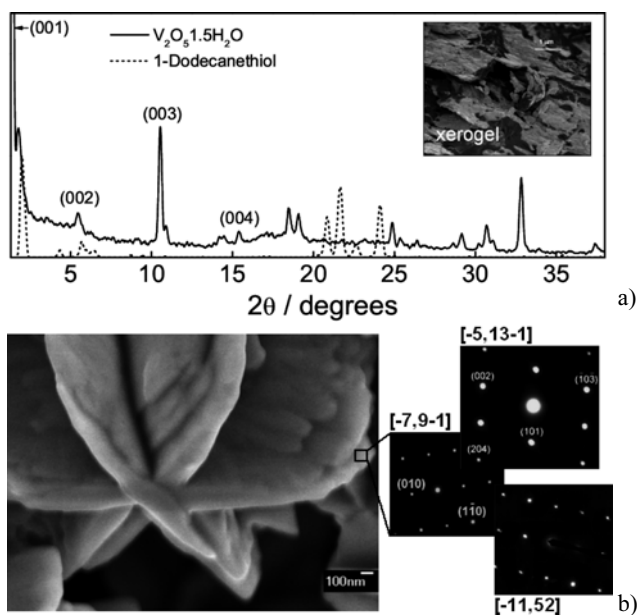


Fig. 2 (a) XRD pattern of both the $V_2O_5 \cdot 1.5H_2O$ xerogel and of a grazing-incidence pattern of a dodecanethiol monolayer FESEM image (*inset*) of the lamellar xerogel. (b) FESEM micrograph of an as-synthesized nanostructure. The corresponding SAED patterns (*right*) of an individual platelet along its $[\bar{5}131]$, $[\bar{7}91]$, and $[1152]$ zone normals of the V_6O_{11} phase.

The diffraction pattern of the resulting material is shown in Fig. 2a and is consistent with the intercalation of the thiol into the lamellar matrix (an FESEM image of which is shown *inset*), and indicates that the framework of the host is preserved, coherent with a topotactic reaction. The presence of the thiol contribution within the lamellar nanostructure is clearly discernible by comparison with its monolayer diffraction pattern.

We also observe that this product exhibits a lamellar structure with an interlamellar distance measured to be 0.25 nm, corresponding to one monolayer of dodecanethiol intercalated between the xerogel lamella (interlamellar distance 0.127 nm). There is a notable absence of a high intensity (002) reflection from the xerogel, consistent with its arrangement as a bi-layered product where two vanadate layers are bound by surfactant [9] and this arrangement is stacked periodically back-to-back. Each of the structures consists of a central axis and each axis consists of spokes or platelets that self-assemble into a six-branched structure, as observed in Fig. 3. The platelets homogeneously distribute around the central axis,

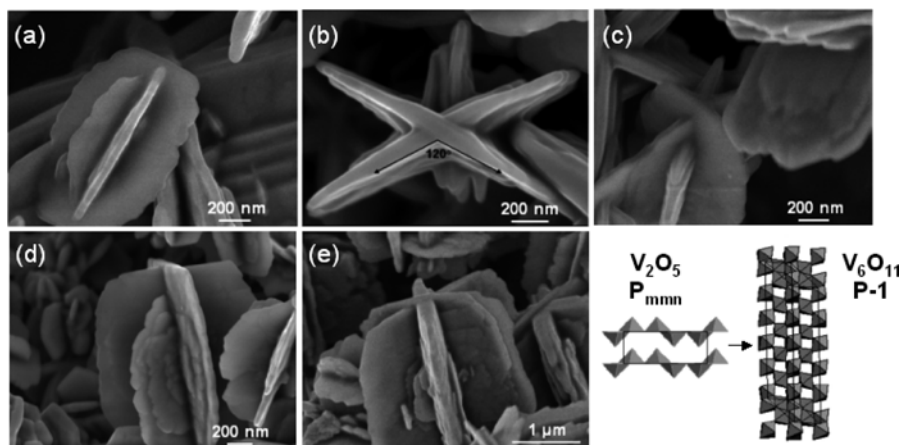


Fig. 3 (a–e) FESEM images of the nucleation of lamellar order and subsequent growth stages of the V_6O_{11} nanostructures, (f) schematic difference between V_2O_5 (SG = P_{mmm}) and V_6O_{11} (SG = $P\bar{1}$) unit cell structures constructed with VO_3 units.

forming the rotationally symmetric architecture. The angle between each pair of adjacent branches is very close to 60° (Fig. 3b). The platelets are grown along the direction perpendicular to the central axis.

The $V_2O_5 \cdot 1.5H_2O$ xerogel is essentially a stack of ribbon-like slabs, which are bi-layers of single V_2O_5 layers consisting of square pyramidal VO_5 units, as depicted in Fig. 3f. These 2D sheets are weakly bound by van der Waals forces and are readily propped open by intercalation species such as dodecanethiol in this instance. Hydrothermal treatment of the thiol-containing xerogel above 450 K induces loss of bound water molecules and recrystallization of the material during thiol-bond weakening. After the determination of a preferred crystalline phase during the initial nucleation stage from the xerogel, the subsequent kinetic growth governs the final architecture of the nanocrystals. Figure 3a–e highlight the principal stages of growth of the structures and evidence their six-fold rotational symmetry, which nucleates progressively. Lamellar rearrangement of the xerogel occurs, and subsequent growth is crystallographically ordered. In the presence of thiols, the resulting plates experience an attachment process due to the capping ability of the surfactant.

The platelets grow along the crystallographically equivalent a axes along the $\pm[1010]$, $\pm[0110]$, and $\pm[1100]$ directions. The V_2O_5 xerogel undergoes a morphotropic transition to V_6O_{11} reminiscent of a reconstructive phase transition [10] where all homologous series V_nO_{2n-1} and V_nO_{2n+1} phases can be ultimately derived from a common disordered polytype hexagonal structure [11]. A long period modulated Magnéli phase is thus formed by the removal of one oxygen layer at every n -th vanadium layer in the direction perpendicular to the $\{211\}$ plane of $VO_2(R)$.

4 Conclusions

In summary, we have successfully synthesized single crystal V_6O_{11} nanostructures from the V_2O_5 xerogel and polymer hybrid nanocomposite. Detailed TEM analyses elucidated the unique single crystal structure and six-fold rotational symmetry of the structures. On cooling, the fraction of disordered sequences of layers in the vanadate xerogel reduce and the intrinsically faulted ordered regions tend to coalesce. Thus, the V_2O_5 xerogel undergoes a morphotropic transition to V_6O_{11} . These types of mechanistic studies may form the basis for controlling morphological geometries of a wide range of nanocrystalline products. Our systematic study of growth parameters in conjunction with detailed structural studies have provided an outline of the shape-evolution process and may be applied to the growth of low-dimensional structures of other materials with layered structure.

Acknowledgements This material is based upon work supported by the Science Foundation Ireland under Grant No. 02/IN.1/172. Support from FONDECYT Grants 1050344, 1030102, 7050081, and 1050788, the University of Chile, and the Universidad Tecnológica Metropolitana and the EU-Network of Excellence PhOREMOST (FP6/2003/IST/2-511616) are also gratefully acknowledged.

References

- [1] P. X. Gao and Z. L. Wang, *Appl. Phys. Lett.* **84**, 2883 (2004).
- [2] N. Soga and M. Senna, *Solid State Ion.* **63–65**, 471 (1993).
- [3] P. Gomez-Romero, *Adv. Mater.* **13**, 163 (2001).
- [4] J. F. Xu, R. Czerw, S. Webster, D. L. Carroll, J. Ballato, and R. Nesper, *Appl. Phys. Lett.* **79**, 1711 (2002).
- [5] C. Gomez-Navarro, P. J. de Pablo, J. Colchero, Y. Fan, M. Burghard, J. Gomez-Herrero, and A. M. Baro, *Nanotechnology* **14**, 134 (2003).
- [6] V. Lavayen, C. O'Dwyer, S. B. Newcomb, M. A. Santa Ana, E. Benavente, G. Gonzalez, and C. M. Sotomayor Torres, *phys. stat. sol. (b)* **243**, 3285 (2006).
- [7] C. O'Dwyer, D. Navas, V. Lavayen, E. Benavente, M. A. Santa Ana, G. Gonzalez, S. B. Newcomb, and C. M. Sotomayor Torres, *Chem. Mater.* **18**, 3016 (2006).
- [8] D. B. McWhan, M. Marezio, J. P. Remeika, and P. D. Dernier, *Phys. Rev. B* **10**, 490 (1974).
- [9] C. O'Dwyer, V. Lavayen, S. B. Newcomb, M. A. Santa Ana, E. Benavente, G. Gonzalez, and C. M. Sotomayor Torres, *Electrochem. Solid-State Lett.* **10**, A111 (2007).
- [10] P. Tolédano and V. Dmitriev, *Reconstructive Phase Transitions* (World Scientific, Singapore, 1996).
- [11] H. Katzke, P. Tolédano, and W. Depmeier, *Phys. Rev. B* **68**, 024109 (2003).